

# Generation of intense dissipation in high Reynolds number turbulence

Dhawal Buaria,<sup>1,2,\*</sup> Alain Pumir,<sup>3,2</sup> and Eberhard Bodenschatz<sup>2,4</sup>

<sup>1</sup>*Tandon School of Engineering, New York University, New York, NY 11201, USA*

<sup>2</sup>*Max Planck Institute for Dynamics and Self-Organization, 37077 Göttingen, Germany*

<sup>3</sup>*Laboratoire de Physique, ENS de Lyon, Université de Lyon 1 and CNRS, 69007 Lyon, France*

<sup>4</sup>*Institute for Nonlinear Dynamics, University of Göttingen, 37077 Göttingen, Germany*

(Dated: July 6, 2021)

Intense fluctuations of energy dissipation rate in turbulent flows result from the self-amplification of strain rate via a quadratic nonlinearity, with contributions from vorticity (via the vortex stretching mechanism) and pressure-Hessian – which are analyzed here using direct numerical simulations of isotropic turbulence on up to  $12288^3$  grid points, and Taylor-scale Reynolds numbers in the range 140 – 1300. We extract the statistics of various terms involved in the amplification of strain and condition them on the magnitude of strain. We find that strain is self-amplified by the quadratic nonlinearity, and depleted via vortex stretching; whereas pressure-Hessian acts to redistribute strain fluctuations towards the mean-field and hence depletes intense strain. Analyzing the intense fluctuations of strain in terms of its eigenvalues reveals that the net amplification is solely produced by the third eigenvalue, resulting in strong compressive action. In contrast, the self-amplification acts to deplete the other two eigenvalues, whereas vortex stretching acts to amplify them, with both effects canceling each other almost perfectly. The effect of the pressure-Hessian for each eigenvalue is qualitatively similar to that of vortex stretching, but significantly weaker in magnitude. Our results conform with the familiar notion that intense strain is organized in sheet-like structures, which are in the vicinity of, but never overlap with tube-like regions of intense vorticity due to fundamental differences in their amplifying mechanisms.

## I. INTRODUCTION

The dissipation rate of kinetic energy,  $\epsilon$ , defined as:

$$\epsilon = 2\nu S_{ij}S_{ij} \text{ , where } S_{ij} = \frac{1}{2} \left( \frac{\partial u_i}{\partial x_j} + \frac{\partial u_j}{\partial x_i} \right) \text{ ,} \quad (1)$$

plays an indispensable role in our understanding of turbulent fluid flows. Here,  $\nu$  is the kinematic viscosity and  $S_{ij}$  is the strain rate tensor (the symmetric part of the velocity gradient tensor  $\partial u_i/\partial x_j$ ). The mean of dissipation rate quantifies the net cascade of energy from large to small scales, manifestly becoming independent of  $\nu$ , as  $\nu \rightarrow 0$  [1–3]. This property, also known as dissipative anomaly, is the central tenet of nearly all turbulence theories and models [1]. However, the fluctuations of dissipation rate (and hence that of strain rate) can be orders of magnitude larger than its mean [4, 5], a phenomena known as intermittency, which renders any mean-field description of turbulence inadequate [1, 6]. Understanding the formation of such intense fluctuations and characterizing their statistical properties has long remained one of the outstanding challenges in turbulence [1, 7].

Understanding the intense fluctuations of dissipation is also directly important from a practical standpoint. For instance, strong strain rates can greatly enhance dispersion of particles and influence mixing of scalars or can adversely affect flame propagation in reacting flows [8–11]. Intense strain also leads to generation of intense vorticity, via the well-known vortex stretching mechanism [12], which in turn influences clustering of inertial particles [13]. In fact, strain and vorticity are

---

\* dhawal.buaria@nyu.edu

not independent and their coupling implicitly encodes all the multiscale interactions in the flow [14–16]. While much attention has been recently given to understand this interaction in light of vorticity amplification [15–17] and energy cascade across scales [18, 19], in the current work, we present a complementary investigation focusing on amplification of strain (and hence dissipation rate).

The key mechanisms controlling amplification of strain can be readily identified by writing its transport equation (as derived from the incompressible Navier-Stokes equations):

$$\frac{DS_{ij}}{Dt} = -S_{ik}S_{kj} - \frac{1}{4}(\omega_i\omega_j - \omega_k\omega_k\delta_{ij}) - \Pi_{ij} + \nu\nabla^2 S_{ij} \quad (2)$$

where  $\boldsymbol{\omega} = \nabla \times \mathbf{u}$  is the vorticity vector and  $\Pi_{ij} = \frac{1}{\rho} \frac{\partial^2 P}{\partial x_i \partial x_j}$  is the pressure Hessian tensor. The first term on the r.h.s. of Eq. (2) captures the self-amplification of strain, which by itself could lead to a finite time singularity. The second term captures the influence of vorticity and essentially the feedback of vortex stretching on strain itself. The third term involving pressure-Hessian represents the influence of non-local effects via the pressure field, and hence couples the entire state of the flow. This nonlocal dependence is readily seen by taking the trace of Eq. (2), leading to the Poisson equation:

$$\Pi_{ii} = \nabla^2 P / \rho = (\omega_i\omega_i - 2S_{ij}S_{ij})/2. \quad (3)$$

The final (linear) term in Eq. (2) represents the viscous diffusion of strain.

In this work, our main goal is to investigate various amplification mechanisms leading to the formation intense strain and hence dissipation. To this end, we analyze the statistics of the (inviscid) nonlinear terms in Eq. (2), in particular by conditioning them on magnitude of strain. One of the implicit goals is to also identify and understand which (inviscid) mechanism(s) possibly contribute in preventing an unbounded growth of strain [15]. We utilize data from high-resolution direct numerical simulations (DNS) of isotropic turbulence in periodic domains, which is the most efficient numerical tool to study the small-scale properties of turbulence. Another important purpose of the current study is also to understand the effect of increasing Reynolds number. With that in mind, we utilize a massive DNS database with Taylor-scale Reynolds number  $R_\lambda$  ranging from 140 to 1300 on grid sizes going up to  $12288^3$ , with particular attention on resolving the small-scales and hence the extreme fluctuations accurately [15–17].

To get insight on the formation of intense strain we compute various statistics related to strain amplification, conditioned on magnitude of strain. We find that the self-amplification solely drives the growth of intense fluctuations, whereas vortex stretching and pressure Hessian terms act to attenuate this growth. By decomposing various contributions in the eigenframe of strain tensor, we further show that this amplification and attenuation predominantly occurs for the most negative eigenvalue, signifying intense strain events correspond to strong compressive motion. In contrast, the other two eigenvalues are amplified by the vortex stretching mechanism and depleted by the self-amplification term, with both these mechanisms canceling each other almost perfectly. The effect of the pressure Hessian, qualitatively similar to that of vortex stretching, is to weakly amplify these two eigenvalues. The structure of the nonlinearities discussed here is consistent with the notion that regions of intense strain are organized in sheet-like structures [20, 21], which are unlikely to be colocated with regions of intense vorticity organized in tube-like structures [22, 23] – underscoring the importance of non-local interactions between strain and vorticity in amplifying gradients [15, 16].

The rest of the manuscript is organized as follows. In § II, we briefly provide the details pertaining to DNS database utilized in this work. The various nonlinearities controlling the amplification of strain are investigated in § III, in particular by analyzing their statistics on magnitude of strain.

In § III C, the various contributions are further analyzed in the eigenbasis of strain tensor. Finally, we summarize our results in § IV.

## II. NUMERICAL APPROACH AND DATABASE

The data utilized here are the same as in recent works [5, 15–17, 24] and are generated using direct numerical simulations (DNS) of incompressible Navier-Stokes equations, for the canonical setup of isotropic turbulence in a periodic domain. The simulations are carried out using highly accurate Fourier pseudo-spectral methods with second-order Runge-Kutta integration in time, and the large scales are forced numerically to achieve statistical stationarity. A key characteristic of our data is that we have achieved a wide range of Taylor-scale Reynolds number  $R_\lambda$ , going from 140 – 1300, while maintaining excellent small-scale resolution on grid sizes of going up to  $12288^3$ . The resolution is as high as  $k_{\max}\eta \approx 6$ , where  $k_{\max} = \sqrt{2}N/3$ , is the maximum resolved wavenumber on a  $N^3$  grid, and  $\eta$  is the Kolmogorov length scale. Convergence with respect to resolution and statistical sampling has been adequately established in previous works [15, 17]. We summarize the DNS database and the simulation parameters in Table I.

$R_\lambda$	$N^3$	$k_{\max}\eta$	$T_E/\tau_K$	$T_{sim}$	$N_s$
140	$1024^3$	5.82	16.0	$6.5T_E$	24
240	$2048^3$	5.70	30.3	$6.0T_E$	24
390	$4096^3$	5.81	48.4	$2.8T_E$	35
650	$8192^3$	5.65	74.4	$2.0T_E$	40
1300	$12288^3$	2.95	147.4	$20\tau_K$	18

TABLE I. Simulation parameters for the DNS runs used in the current work: the Taylor-scale Reynolds number ( $R_\lambda$ ), the number of grid points ( $N^3$ ), spatial resolution ( $k_{\max}\eta$ ), ratio of large-eddy turnover time ( $T_E$ ) to Kolmogorov time scale ( $\tau_K$ ), length of simulation ( $T_{sim}$ ) in statistically stationary state and the number of instantaneous snapshots ( $N_s$ ) used for each run to obtain the statistics.

## III. STATISTICS CONDITIONED ON STRAIN/DISSIPATION

In order to quantify the intensity of strain, we consider the quantity  $\Sigma$  defined as

$$\Sigma = 2S_{ij}S_{ij} \quad (4)$$

which is simply the dissipation rate without the viscosity, i.e.,  $\Sigma = \epsilon/\nu$ . The benefit of directly using  $\Sigma$  is that its mean defines the Kolmogorov time scale  $\tau_K$ , i.e.,  $\langle \Sigma \rangle = 1/\tau_K^2$  and from homogeneity is also equal to the mean of enstrophy, i.e.,  $\langle \Sigma \rangle = \langle \Omega \rangle$ , where  $\Omega = \omega_i\omega_i$ . From Eq. (2), the following transport equation for  $\Sigma$  can be derived:

$$\frac{1}{4} \frac{D\Sigma}{Dt} = -S_{ij}S_{jk}S_{ki} - \frac{1}{4}\omega_i\omega_jS_{ij} - S_{ij}\Pi_{ij} + \nu S_{ij}\nabla^2 S_{ij}, \quad (5)$$

where the term  $\omega_i\omega_jS_{ij}$ , which leads to production of enstrophy when considering vorticity transport equation [17], clearly demonstrates the feedback of vortex stretching on amplification of strain.

In statistically stationary isotropic turbulence, as considered in this work, the mean of the l.h.s. of Eq. (5) is zero. For the terms on r.h.s., it is known that [7, 25]:

$$\langle S_{ij}\Pi_{ij} \rangle = 0 \quad (6)$$

$$-\langle S_{ij}S_{jk}S_{kj} \rangle = \frac{3}{4}\langle \omega_i\omega_jS_{ij} \rangle \quad (7)$$

Utilizing these relations, the averaging of Eq. (5) leads to:

$$\langle S_{ij}S_{jk}S_{ki} \rangle = \frac{3}{2}\nu \langle S_{ij}\nabla^2 S_{ij} \rangle \quad (8)$$

which gives a simple balance between inviscid production and viscous dissipation of strain. Since  $\langle \omega_i \omega_j S_{ij} \rangle$  is known to be positive on average [25], it follows that  $-\langle S_{ij}S_{jk}S_{ki} \rangle > 0$ , therefore implying generation of strain via a self-amplification mechanism. While the results in Eqs. (7)-(8), hold on average for the entire flow field, they do not imply any particular relation when considering the same statistics conditioned on  $\Sigma$  (which is required to isolate the extreme events from the mean-field). In the following, we investigate the role of various terms in Eq. (5) conditioned on  $\Sigma$ .

### A. Strain self-amplification and vortex stretching

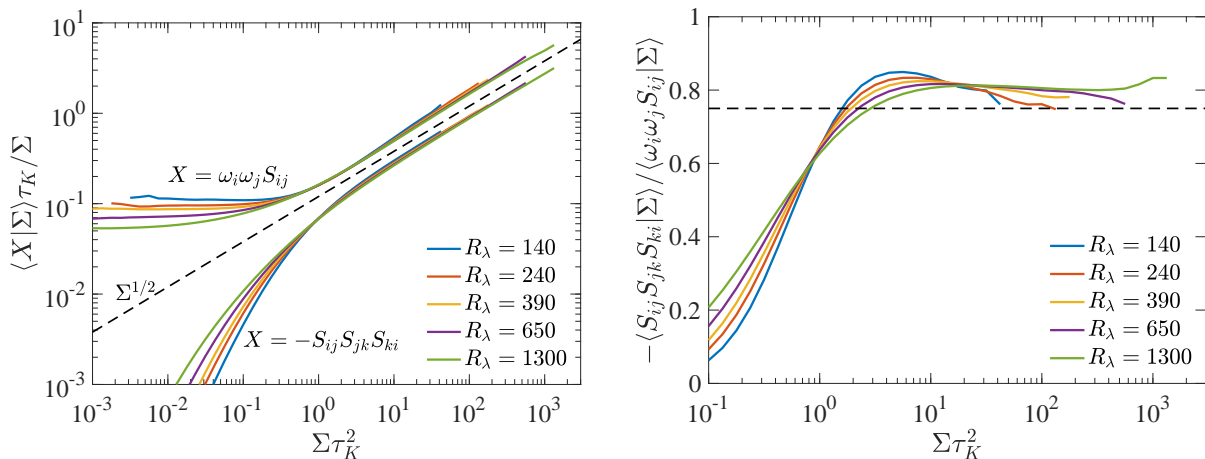


FIG. 1. (a) Conditional expectations (given  $\Sigma$ ) of the strain self-amplification and vortex stretching terms, for various  $R_\lambda$ . All quantities are normalized by Kolmogorov time scale  $\tau_K = \langle \Sigma \rangle^{-1/2}$ . The black dashed line indicates the power-law  $\Sigma^{1/2}$ . (b) The ratio of conditional strain self-amplification and vortex stretching terms. The horizontal dashed line indicates the value 3/4, corresponding to the ratio of unconditional averages as given by Eq. (7).

In this subsection, we analyze the contributions from the self-amplification and vortex stretching terms when conditioned on magnitude of strain, i.e., respectively  $-\langle S_{ij}S_{jk}S_{ki} | \Sigma \rangle$  and  $\langle \omega_i \omega_j S_{ij} | \Sigma \rangle$ . Figure 1a shows both terms, divided by  $\Sigma$  for convenience and for various  $R_\lambda$ . All quantities are appropriately non-dimensionalized by  $\tau_K$ , which allows us to demarcate the strength of events with respect to the mean-field. The main observation is that both the plotted quantities in Fig. 1a scale as  $\Sigma^{1/2}$  (marked by black dashed line) for events stronger than the mean ( $\Sigma \tau_K^2 \gtrsim 1$ ), which implies the conditional expectations themselves scale as  $\Sigma^{3/2}$  – consistent with simple dimensional argument. Moreover, the dependence on  $R_\lambda$  is very weak (especially as  $R_\lambda$  increases), suggesting an asymptotic state has likely been reached.

It should be noted that the magnitude of the vortex stretching term (which depletes strain) is larger, but its net contribution is still lower than the self-amplification term due to the factor of 1/4 in Eq. (5). To further investigate their relative contributions, Fig. 1b shows the ratio of their conditional expectations for various  $R_\lambda$ . For extreme events of strain, we observe that the ratio seemingly asymptotes to a constant value of about 0.8, which is different and slightly larger than

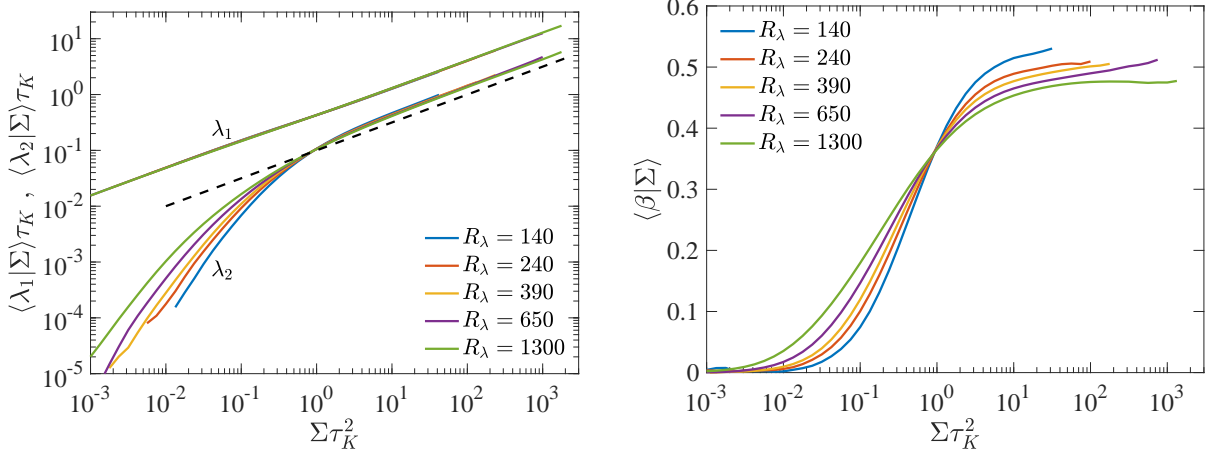


FIG. 2. Conditional expectations (given  $\Sigma$ ) of (a) first two eigenvalues of strain tensor, (b) the ratio  $\beta$  as defined by Eq. (10), for various  $R_\lambda$ . The dashed line in (a) indicates a power law of  $\Sigma^{1/2}$ .

3/4, the value of their unconditional averages. This implies that the overall (negative) contribution of the vortex stretching term is about  $1/(4 \times 0.8) \approx 1/3.2$  times that of the strain self-amplification term, which is slightly smaller than the factor 1/3 valid for the overall field (as seen from Eqs. (5) and (7)).

To better understand the results in Fig. 1, we analyze them further in the eigenframe of strain, as given by its three eigenvalues  $\lambda_i$  (for  $i = 1, 2, 3$ , such that  $\lambda_1 \geq \lambda_2 \geq \lambda_3$ ) and the corresponding eigenvectors  $\mathbf{e}_i$ . Incompressibility imposes  $\lambda_1 + \lambda_2 + \lambda_3 = 0$ , which renders  $\lambda_1$  to be always positive (stretching) and  $\lambda_3$  to be always negative (compressive). It is well known that the second (intermediate) eigenvalue  $\lambda_2$  is positive on average, leading to net production of enstrophy [17, 25, 26]. Using the eigenframe, we can readily show that

$$\Sigma = 2(\lambda_1^2 + \lambda_2^2 + \lambda_3^2), \quad S_{ij}S_{jk}S_{ki} = \lambda_1^3 + \lambda_2^3 + \lambda_3^3 = 3\lambda_1\lambda_2\lambda_3. \quad (9)$$

The power-law behavior of  $-\langle S_{ij}S_{jk}S_{ki} | \Sigma \rangle \sim \Sigma^{3/2}$  (for  $\Sigma \tau_K^2 > 1$ ) suggests that the magnitude of individual eigenvalues of strain would simply scale as  $\Sigma^{1/2}$ . Fig. 2a shows the conditional average of first two eigenvalues, and confirms this expectation (the third eigenvalue, which has the largest magnitude, can be obtained via the incompressibility condition). It can also be seen that  $\lambda_2$  is always positive, but does not scale as  $\Sigma^{1/2}$  for weak strain events ( $\Sigma \tau_K^2 < 1$ ), and instead has a larger exponent. This can be explained by realizing that when the magnitude of strain approaches zero,  $\lambda_2$  would also approach zero, due to strong cancellation between  $\lambda_1$  and  $\lambda_3$ . This expectation is verified in Fig. 2b, which shows the quantity  $\beta$  [17, 26], defined as:

$$\beta = \sqrt{6} \frac{\lambda_2}{\sqrt{\lambda_1^2 + \lambda_2^2 + \lambda_3^2}} = \sqrt{12} \frac{\lambda_2}{\Sigma^{1/2}} \quad (10)$$

conditioned on  $\Sigma$ . It can be observed that  $\beta \rightarrow 0$  when  $\Sigma \rightarrow 0$ , and only for  $\Sigma \tau_K^2 > 1$ , it becomes a constant (provided the  $R_\lambda$  is sufficiently high). It is worth noting that this overall trend for  $\lambda_2$  also explains the behavior of strain self-amplification term in Fig. 1a for the region  $\Sigma \tau_K^2 < 1$ .

The vortex stretching term can be expressed in the eigenframe of strain as:

$$\omega_i \omega_j S_{ij} = \lambda_i (\mathbf{e}_i \cdot \boldsymbol{\omega})^2 = \Omega \lambda_i (\mathbf{e}_i \cdot \hat{\boldsymbol{\omega}})^2, \quad (11)$$

with  $\hat{\boldsymbol{\omega}} = \boldsymbol{\omega}/|\boldsymbol{\omega}|$ , highlighting the importance of the alignment of vorticity with strain-eigenvectors (along with magnitude of vorticity and strain) in determining the efficacy of vortex stretching (or

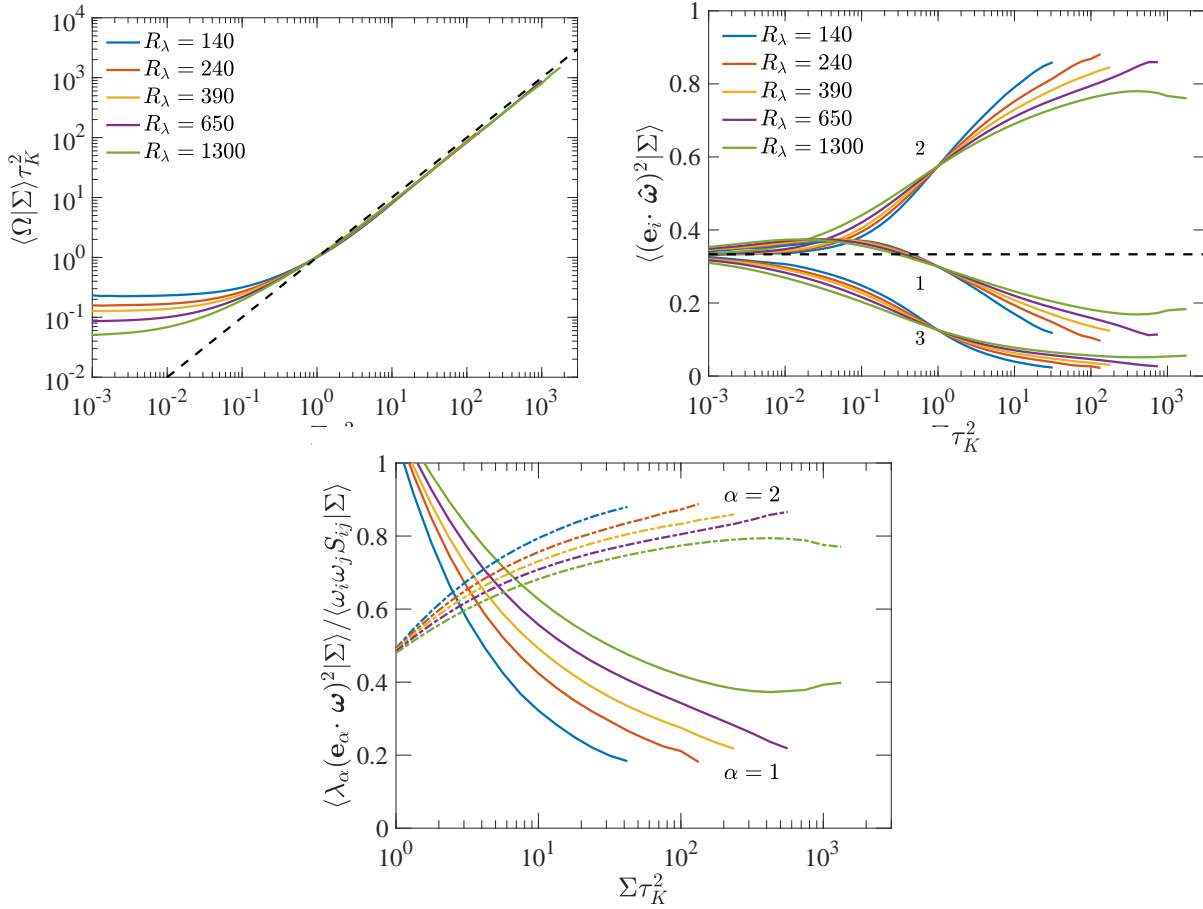


FIG. 3. Conditional expectations (given  $\Sigma$ ) of (a) enstrophy,  $\Omega$ , (b) second moment of alignment cosines between vorticity and eigenvectors of strain, and (c) the relative contribution to the vortex stretching term from the first two eigendirections of strain, for various  $R_\lambda$ . The dashed line in (a) corresponds to a power-law of  $\Sigma^1$ . The dashed line in (b) is at  $1/3$ , corresponding to a uniform distribution of alignment cosines (indicating lack of any preferential alignment).

strain depletion in this case) [7, 26]. The conditional expectation of enstrophy is shown in Fig. 3a, exhibiting the same qualitative behavior as  $\omega_i \omega_j S_{ij}$  in Fig. 1a. For intense strain events ( $\Sigma \tau_K^2 > 1$ ), we find that  $\langle \Omega | \Sigma \rangle \sim \Sigma$ , suggesting a simple causal relation that intense strain produces equally intense vorticity (as anticipated from vortex stretching). On the other hand, for weak strain events ( $\Sigma \tau_K^2 < 1$ ), the conditional average is constant, suggesting a lack of correlation between strain and vorticity [7, 17] (which is also reflected in the behavior of  $\omega_i \omega_j S_{ij}$  in Fig. 1a).

Figure 3b shows the conditional expectation of the second moment of alignment cosines, i.e.,  $\langle (\mathbf{e}_i \cdot \hat{\boldsymbol{\omega}})^2 | \Sigma \rangle$ , which are individually bounded between 0 and 1, respectively for orthogonality and perfect alignment, and are equal to  $1/3$  for no preferential alignment (corresponding to a uniform distribution of the cosine). Additionally, the three alignment cosines (for  $i = 1, 2, 3$ ) also add up to unity. Overall, the alignments follow the same trend as when conditioned on vorticity (see Fig. 3d in [17]), i.e., in regions of intense strain ( $\Sigma \tau_K^2 > 1$ ), vorticity is strongly aligned with  $\mathbf{e}_2$  and preferentially orthogonal to both  $\mathbf{e}_{1,3}$  (more so with  $\mathbf{e}_3$ ). Whereas for  $\Sigma \tau_K^2 \ll 1$ , the alignments approach  $1/3$ , reaffirming a lack of correlation between strain and vorticity. However, unlike when conditioned on vorticity (in [17]), the alignments in Fig. 3b show a significant  $R_\lambda$ -dependence. The emergence of a plateau-like behavior for  $R_\lambda = 1300$  suggests an asymptotic state would likely be

reached if  $R_\lambda$  is further increased.

Fig. 3c shows the relative contributions of each eigenvalue to the overall vortex stretching term. We only show contributions corresponding to first and second eigenvalues, which are both positive). The (negative) contribution for the third eigenvalue is quite small, and can be evaluated by realizing that all three contributions add up to unity. Interestingly, we notice that the contribution from the second eigenvalue is significantly stronger than that from the first eigenvalue, and accounts for most of vortex stretching. The difference between the two gradually decreases with  $R_\lambda$ , but nevertheless, even at the highest  $R_\lambda$  ( $= 1300$ ), the second eigenvalue contributes to nearly 80% of the net vortex stretching. The results on alignments in Fig. 3b, combined with these indicate a strong structural difference between regions of intense strain and vorticity. In regions of intense vorticity, even though vorticity is strongly aligned with the second eigenvector, the first eigenvalue contributes more significantly to overall vortex stretching [17]. This difference can be explained by realizing that the relative magnitude of  $\lambda_2$  itself is significantly smaller in regions of intense vorticity (compared to regions of intense strain) [17].

From a structural point of view, the above results are consistent with the notion that intense vorticity is arranged in tube-like structures, whereas intense strain is arranged in sheet-like structures [20]. In both scenarios, vorticity has the propensity to align with second eigenvector of strain. However, for the case of vortex tubes, the corresponding magnitude of second eigenvalue is significantly smaller [17]. We will discuss more about this later in § 3(c).

## B. Role of pressure Hessian

We next consider the contribution of pressure Hessian to generation of strain. To this end, Fig. 4a shows the conditional average  $\langle S_{ij}\Pi_{ij}|\Sigma\rangle$ , once again divided by  $\Sigma$  for convenience. Since the corresponding unconditional average is zero, the conditional average cannot keep the same sign for all values of  $\Sigma$ . Figure 4a shows that for events stronger than the mean ( $\Sigma\tau_K^2 \gtrsim 1$ ) this quantity is positive, and thus leads to depletion of strain (due to the negative sign associated with the term in Eq. (5)), and vice-versa for events weaker than the mean. Thus, the non-local pressure field on average acts to redistribute the strain fluctuations towards its mean amplitude [27]. It should be further noted, that for intense strain, the conditional average scales once again as  $\Sigma^{3/2}$ , whereas for weak strain events it scales as  $\Sigma^1$  – albeit with a much smaller pre-factor (in both regimes) when compared to the strain self-amplification or vortex stretching terms.

While the overall contribution of the pressure field is to drive strain fluctuations towards the mean field, it is once again instructive to analyze the individual contributions in the eigenframe of strain tensor – where the strain-pressure Hessian correlation can be rewritten as:

$$S_{ij}\Pi_{ij} = \lambda_i \tilde{\Pi}_i \quad (12)$$

where  $\tilde{\Pi}_\alpha = \mathbf{e}_\alpha^T \mathbf{\Pi} \mathbf{e}_\alpha$  is the projection of pressure Hessian tensor along the eigenvector  $\mathbf{e}_\alpha$  of the strain. and repeated  $\alpha$  does not imply summation (a convention which we will adhere to henceforth). Note that the eigenvalues of strain can also be defined in a similar way:  $\lambda_\alpha = \mathbf{e}_\alpha^T \mathbf{S} \mathbf{e}_\alpha$ . We also introduce the eigenframe of the pressure Hessian tensor, defined by eigenvalues  $\lambda_i^p$  (for  $i = 1, 2, 3$  and also arranged in descending order) and corresponding eigenvectors  $\mathbf{e}_i^p$ , leading to:

$$\tilde{\Pi}_i = \lambda_j^p (\mathbf{e}_i \cdot \mathbf{e}_j^p)^2, \quad \text{and} \quad (13)$$

$$S_{ij}\Pi_{ij} = \lambda_i \lambda_j^p (\mathbf{e}_i \cdot \mathbf{e}_j^p)^2 \quad (14)$$

Note  $\sum_\alpha \lambda_\alpha^p = \nabla^2 P / \rho = (\Omega - \Sigma) / 2$  (utilizing Eq. (3)). Thus, from the result in Fig. 3, i.e.,  $\langle \Omega | \Sigma \rangle \simeq c \Sigma^1$  (with  $c \lesssim 1$ ), it follows that in regions of intense strain the sum of three eigenvalues

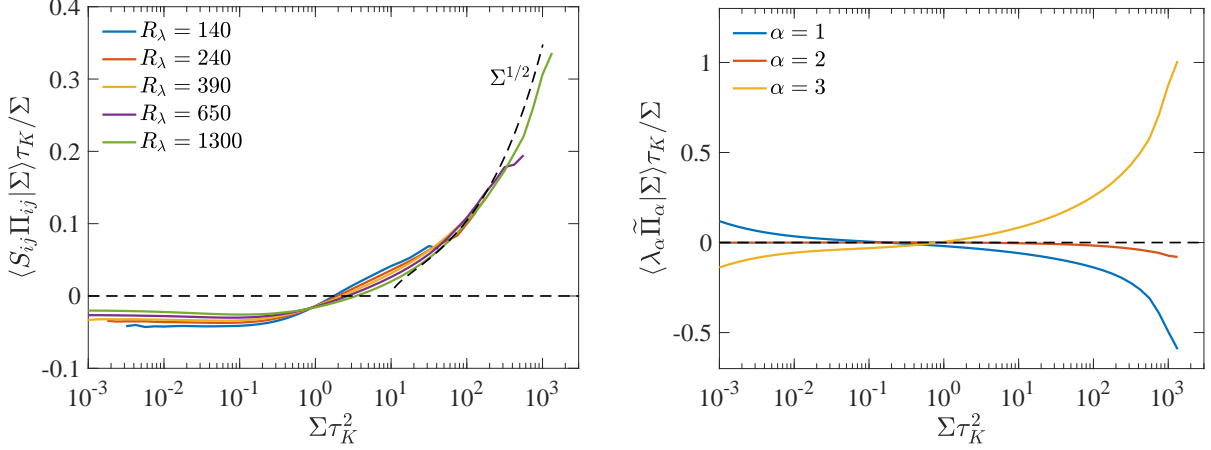


FIG. 4. Conditional expectations (given  $\Sigma$ ) of (a) strain and pressure-Hessian correlation for various  $R_\lambda$ , and (b) the individual contributions in the eigenframe of strain, as defined by Eq. (12), for only  $R_\lambda = 1300$ . The expectations are once again divided by  $\Sigma$ , and all quantities are non-dimensionalized by  $\tau_K$ .

is overall small in magnitude with a negative sign – which in turn suggests a dominant role of  $\lambda_3^p$ , which we analyze next.

Figure 4b shows the breakup of individual contributions to strain-pressure Hessian correlation as given in Eq. (13), i.e.,  $\langle \lambda_\alpha \tilde{\Pi}_\alpha | \Sigma \rangle$  (we recall again that no summation is implied over  $\alpha$ ). It is observed that the dominant positive contribution comes from the third eigenvalue of strain (and hence leads to depletion of strain), whereas the other two contributions are negative (leading to amplification of strain). These trends can be simply explained from Eq. (14) by assuming that the alignments  $(\mathbf{e}_i \cdot \mathbf{e}_j^p)^2$  are all 1/3 (corresponding to lack of any preferential alignment) – leading to  $\lambda_\alpha \tilde{\Pi}_\alpha = \lambda_\alpha \sum_\alpha \lambda_\alpha^p = \lambda_\alpha \nabla^2 P / \rho$ . Since  $\nabla^2 P$  is slightly negative for  $\Sigma \tau_K^2 > 1$ , it follows that  $\lambda_\alpha \tilde{\Pi}_\alpha$  has the opposite sign as that of  $\lambda_\alpha$ , consistent with Fig. 4b.

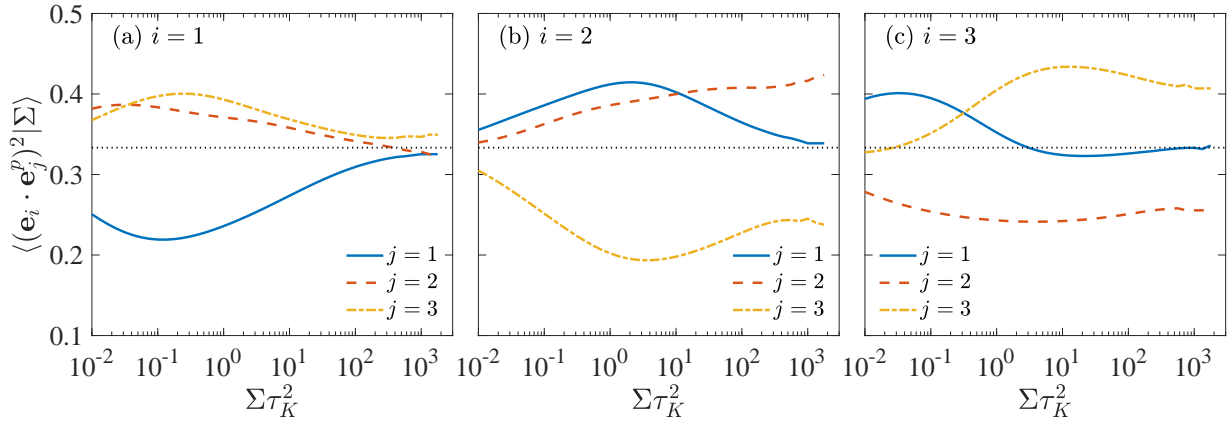


FIG. 5. Conditional expectations (given  $\Sigma$ ) of the alignment cosines between eigenvectors of strain and pressure Hessian, respectively  $\mathbf{e}_i$  and  $\mathbf{e}_j^p$ .

An important assumption in the argument above was the lack of any preferential alignment between the eigenvectors of strain and those of pressure Hessian. Fig. 5 shows the conditional second moments of various alignment cosines, i.e.,  $\langle (\mathbf{e}_i \cdot \mathbf{e}_j^p)^2 | \Sigma \rangle$ . Note, similar to alignment cosines



between vorticity and strain, the alignment cosines for strain and pressure Hessian for any fixed value of  $i$  (or  $j$ ) add up to unity. Additionally, they are all individually bounded between 0 and 1, for orthogonal and perfect alignment respectively; whereas for non-preferential alignment the averages would be  $1/3$  (corresponding to uniform random distribution). Fig. 5 reveals that the deviation of all the alignments from  $1/3$  is very small, therefore excluding any strong alignments between the two sets of eigenvectors. This is to be contrasted with the strong alignment observed between vorticity and strain in Fig. 3b.

### C. Budget of nonlinear terms and strain decomposition

Following upon the results in previous subsections, Fig. 6a compares the contributions of various nonlinear (inviscid) terms on the r.h.s. of Eq. (5) (note that the viscous term is simply the negative of the net contribution of all the inviscid terms). All the terms are now normalized by  $\Sigma^{3/2}$ , and clearly show a plateau for  $\Sigma\tau_K^2 > 1$ . As expected, the dominant positive contribution comes from the strain self-amplification term, whereas the vortex stretching term is negative and significantly smaller in magnitude. The contribution from pressure Hessian term is also negative for  $\Sigma\tau_K^2 \gtrsim 1$  and even smaller in magnitude. To get more insight on the balance of terms in Eq. (5), Fig. 6b shows the data only for  $R_\lambda = 1300$ , including the resulting sum between various terms.

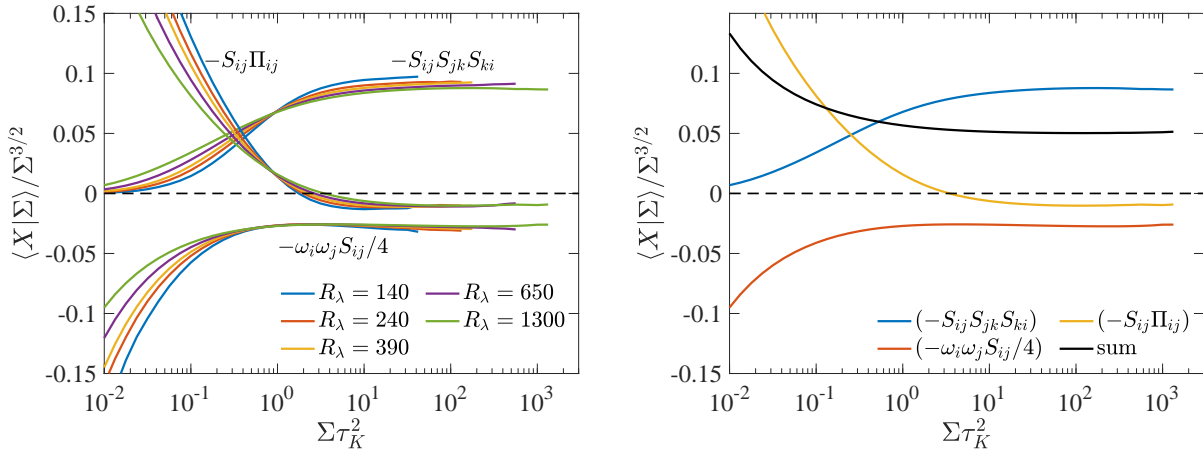


FIG. 6. (a) Conditional expectations (given  $\Sigma$ ) of various nonlinear (inviscid) terms on the r.h.s. of Eq. (5), for various  $R_\lambda$ . All quantities are normalized by  $\Sigma^{3/2}$  revealing a plateau like behavior for  $\Sigma\tau_K^2 > 1$ . The same quantities are shown in (b) for  $R_\lambda = 1300$ , to highlight the combined contributions of the terms.

While the overall contribution of various inviscid terms in generating intense strain, as illustrated in Fig. 6, was relatively straightforward, a more complex picture emerges when considering amplification of individual eigenvalues of strain. To this end, we consider the transport equation for each eigenvalue [28, 29]:

$$\frac{D\lambda_\alpha}{Dt} = -\lambda_\alpha^2 + \frac{\Omega}{4} [1 - (\mathbf{e}_\alpha \cdot \hat{\boldsymbol{\omega}})^2] - \tilde{\Pi}_\alpha + \text{viscous term} \quad (15)$$

Multiplying both sides by  $\lambda_\alpha$  leads to the equation:

$$\frac{1}{2} \frac{D\lambda_\alpha^2}{Dt} = -\lambda_\alpha^3 + \frac{1}{4} \Omega \lambda_\alpha [1 - (\mathbf{e}_\alpha \cdot \hat{\boldsymbol{\omega}})^2] - \lambda_\alpha \tilde{\Pi}_\alpha + \text{viscous terms.} \quad (16)$$

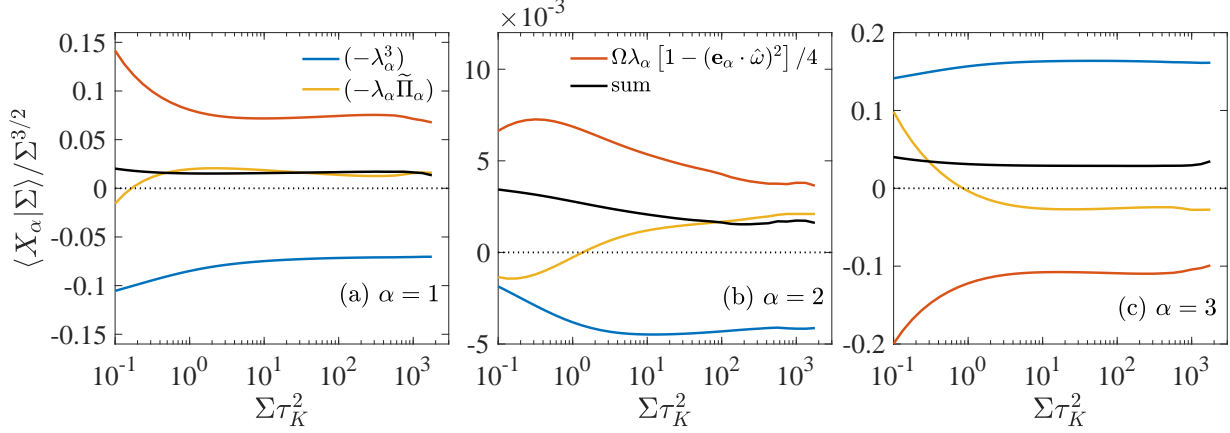


FIG. 7. Conditional expectations of the various inviscid terms in Eq. (16) for (a)  $i = 1$ , (b)  $i = 2$ , and (c)  $i = 3$  (note that repeated indices do not imply summation). All quantities have been normalized by  $\Sigma^{3/2}$ . The legend in (a) and (b) is common to all figures.

providing the individual breakups for Eq. (5), since  $\Sigma = 2 \sum_{\alpha} \lambda_{\alpha}^2$ . Note that the individual eigenvalues now have a direct contribution from vorticity, from the term  $\Omega \lambda_{\alpha}$ , which sums up to zero in Eq. (5) due to incompressibility. This leads to a more involved interplay between strain self-amplification and vortex stretching at the level of individual eigenvalues, than for the total strain in Fig. 6.

Since the first two eigenvalues of strain,  $\lambda_1$  and  $\lambda_2$ , are positive, it follows that the self-amplification term  $-\lambda_{\alpha}^3$ , leads to depletion instead of actual amplification; whereas the contribution due to vortex stretching is overall positive and leads to amplification (since  $1 - (\mathbf{e}_{\alpha} \cdot \hat{\boldsymbol{\omega}})^2 > 0$ ). In contrast, for  $\lambda_3$ , which is negative, the amplification originates from  $-\lambda_3^3$ , and vortex stretching leads to depletion. The sign of the pressure Hessian term,  $-\lambda_{\alpha} \tilde{\Pi}_{\alpha}$  will also be the same as that of  $\lambda_{\alpha}$  (as shown in Fig. 4), and thus would amplify  $\lambda_1$  and  $\lambda_2$ , but deplete  $\lambda_3$ . These expectations are all qualitatively confirmed in Fig. 7, which shows the conditional averages of various terms for each eigenvalue, conditioned on  $\Sigma$  and normalized by  $\Sigma^{3/2}$ . Note, the individual contributions shown in Fig. 7a-c sum up to the terms shown in Fig. 6b. Quantitatively, we find two main trends. For the case of  $\lambda_1$  and  $\lambda_2$ , in Fig. 7a and b respectively, the contributions from self-amplification and vortex stretching terms approximately cancel each other (for  $\Sigma \tau_K^2 > 1$ ), and the net nonlinear amplification almost entirely results from the pressure Hessian term. For  $\lambda_3$ , in Fig. 7c, there is significant cancellation between the self-amplification and vortex stretching terms (and the pressure Hessian term now aids in depletion), but the self-amplification overall dominates.

Thus, the following picture of strain amplification emerges. The self-amplification of strain only occurs along the third eigendirection, i.e. via self-compressive motion, whereas the same mechanism depletes the first two eigenvalues. On the other hand, as strain acts to amplify vorticity (via vortex stretching), the feedback leads to amplification of the first two eigenvalues (which could further aid in vorticity amplification), but leads to depletion of the third eigenvalue. The net result is such that these two effects nearly balance each other for the first two eigenvalues, but the self-amplification prevails for the third eigenvalue. Thus, overall these terms only act to make  $\lambda_3$  more negative (and thus produce strong compressive motion). In this context, the pressure Hessian term acts to deplete the third eigenvalue, and in turn amplify the first two, qualitatively producing a similar effect as vortex stretching.

These results clearly demonstrate that the generation of intense strain differs in crucial aspects compared to generation of intense vorticity [7, 17]. While vortex stretching solely enables generation

of intense vorticity, it also acts to deplete strain at the same spatial location. This suggests that the local maximas of vorticity and strain are never likely to collocated, which has been confirmed in DNS [5, 20, 21] and also corroborated by a simple vortex tube calculation [23]. At the same time, regions of intense strain and vorticity also have to be sufficiently ‘nearby’ and correlated, since strain and vorticity are coupled via the Biot-Savart relation [14, 15]. This is also consistent with observations from DNS, which show that intense strain is arranged in sheet-like structures neighboring tube-like regions of intense vorticity [5]. Finally, these structural differences are in turn consistent with how vorticity-strain correlations differ between regions of intense strain and vorticity. Thus, analyzing the non-local relation between strain and vorticity could be vital to understand their amplification [15, 16] and also could provide a quantitative reasoning as to why vorticity is more intermittent than strain [5].

#### IV. CONCLUSION

In this work, we have utilized a massive DNS database of stationary isotropic turbulence with Taylor-scale Reynolds number in the range 140 – 1300 to analyze the nonlinear mechanisms responsible for generation of extreme events of energy dissipation (and hence strain rate), identified by  $\Sigma = 2S_{ij}S_{ij}$ , where  $S_{ij}$  is the strain-rate tensor. We have investigated the three nonlinear processes involved in the transport equation for  $\Sigma$  (see Eq. (5)), viz., the strain self-amplification, vortex stretching and strain-pressure Hessian correlation, by analyzing their statistics conditioned on  $\Sigma$ . We find that the overall amplification of strain comes from the strain-self amplification term only, whereas the other two terms act to deplete intense strain events. Remarkably, the dependence of various conditional averages on  $\Sigma$  follows a simple dimensional consideration.

The three mechanisms are further analyzed in the eigenbasis of strain tensor, defined by its eigenvalues  $\lambda_i$  and eigenvectors  $\mathbf{e}_i$  (for  $i = 1, 2, 3$ ), revealing a more complex picture. Since  $\lambda_1$  is always positive and  $\lambda_2$  is positive on average, it follows that the self-amplification term in fact leads to depletion for these eigenvalues, whereas the vortex stretching and pressure Hessian terms lead to amplification. Surprisingly, the self-amplification and vortex stretching terms cancel each other and the net amplification is solely provided by the pressure Hessian term. In contrast, the behavior of all these terms for the third eigenvalue (which is always negative) is similar to that of total strain, revealing that extreme events of strain result from strong self-compressive action. Our results are consistent with the notion that regions of intense strain are arranged in sheet-like structures, in the vicinity of, but never collocated with regions of tube-like intense vorticity [5, 20, 21, 23]. In this context, analyzing the non-local relation between strain and vorticity would be crucial in understanding their amplification [14–16] and could also shed light on the long standing mystery of why vorticity is more intermittent than strain.

$X$	$c_X \Sigma^{1/2}$	$X$	$c_X \Sigma^1$	$X$	$c_X \Sigma^{3/2}$	$X$	$c_X \Sigma^{3/2}$	$X$	$c_X \Sigma^{3/2}$
$\lambda_1$	0.412	$\lambda_1^2$	0.173	$\lambda_1^3$	0.074	$\lambda_1(\mathbf{e}_1 \cdot \boldsymbol{\omega})^2$	0.042	$\lambda_1 \tilde{\Pi}_1$	0.013
$\lambda_2$	0.138	$\lambda_2^2$	0.024	$\lambda_2^3$	0.004	$\lambda_2(\mathbf{e}_2 \cdot \boldsymbol{\omega})^2$	0.090	$\lambda_2 \tilde{\Pi}_2$	0.002
$\lambda_3$	-0.550	$\lambda_3^2$	0.303	$\lambda_3^3$	-0.167	$\lambda_3(\mathbf{e}_3 \cdot \boldsymbol{\omega})^2$	-0.019	$\lambda_3 \tilde{\Pi}_3$	-0.024
		$\Omega$	0.856	$S_{ij}S_{jk}S_{ki}$	-0.089	$\omega_i \omega_j S_{ij}$	0.113	$S_{ij} \Pi_{ij}$	-0.010

TABLE II. Pre-factors  $c_X$  for the asymptotic scaling of various conditional statistics satisfying  $\langle X|\Sigma \rangle \approx c_X \Sigma^p$  (in the range  $\Sigma/\langle \Sigma \rangle > 1$ ), such that  $X/\Sigma^p$  is dimensionless  $\lambda_i$  and  $\mathbf{e}_i$  are the eigenvalues and eigenvectors of strain tensor respectively.  $\boldsymbol{\omega}$  is the vorticity and  $\Omega = \omega_i \omega_i$ .  $\Pi_{ij}$  is the pressure Hessian tensor, and  $\tilde{\Pi}_i$  is its projection along  $\mathbf{e}_i$ . The results are obtained from the  $R_\lambda = 1300$  data.

Finally, we note that the conditional statistics investigated in this work have very simple power-law dependences on  $\Sigma$  (in the region  $\Sigma/\langle\Sigma\rangle > 1$ ), as deducible from an elementary dimensional consideration. We have listed all such relevant quantities in Table II, which could be valuable in statistical modeling of energy dissipation rate, especially in PDF methods [30] – an exercise left for future work.

## ACKNOWLEDGEMENTS

We are pleased to present this manuscript in the collection honoring the momentous career of Professor Uriel Frisch. We gratefully acknowledge the Gauss Centre for Supercomputing e.V. for providing computing time on the supercomputers JUQUEEN and JUWELS at Jülich Supercomputing Centre (JSC), where the simulations reported in this paper were performed.

- 
- [1] U. Frisch, *Turbulence: the legacy of Kolmogorov* (Cambridge University Press, Cambridge, 1995).
  - [2] K. R. Sreenivasan, “On the scaling of the turbulence energy dissipation rate,” *Phys. Fluids* **27**, 1048–1051 (1984).
  - [3] Y. Kaneda, T. Ishihara, M. Yokokawa, K. Itakura, and A. Uno, “Energy dissipation rate and energy spectrum in high resolution direct numerical simulations of turbulence in a periodic box,” *Phys. Fluids* **15**, L21–L24 (2003).
  - [4] C. Meneveau and K. R. Sreenivasan, “The multifractal nature of turbulent energy dissipation,” *J. Fluid Mech.* **224**, 429–484.
  - [5] D. Buaria, A. Pumir, E. Bodenschatz, and P. K. Yeung, “Extreme velocity gradients in turbulent flows,” *New J. Phys.* **21**, 043004 (2019).
  - [6] K. S. Sreenivasan and R. A. Antonia, “The phenomenology of small-scale turbulence,” *Annu. Rev. Fluid Mech.* **29**, 435–77 (1997).
  - [7] A. Tsinober, *An Informal Conceptual Introduction to Turbulence* (Springer, Berlin, 2009).
  - [8] D. Buaria, B. L. Sawford, and P. K. Yeung, “Characteristics of backward and forward two-particle relative dispersion in turbulence at different Reynolds numbers,” *Phys. Fluids* **27**, 105101 (2015).
  - [9] D. Buaria, M. P. Clay, K. R. Sreenivasan, and P. K. Yeung, “Small-scale isotropy and ramp-cliff structures in scalar turbulence,” *Phys. Rev. Lett.* **126**, 034504 (2021).
  - [10] H. Pitsch and H. Steiner, “Scalar mixing and dissipation rate in large-eddy simulations of non-premixed turbulent combustion,” *Proc. Combust. Inst.* **28**, 41–49 (2000).
  - [11] P. E. Hamlington, A. Y. Poludnenko, and E. S. Oran, “Interactions between turbulence and flames in premixed reacting flows,” *Physics of Fluids* **23**, 125111 (2011).
  - [12] H. Tennekes and J. L. Lumley, *A First Course in Turbulence* (The MIT Press, 1972).
  - [13] S. Sundaram and L. R. Collins, “Collision statistics in an isotropic particle-laden turbulent suspension. Part 1. Direct numerical simulations,” *J. Fluid Mech.* **335**, 75–109 (1997).
  - [14] P. E. Hamlington, J. Schumacher, and W. J. A. Dahm, “Direct assessment of vorticity alignment with local and nonlocal strain rates in turbulent flows,” *Phys. Fluids* **20**, 111703 (2008).
  - [15] D. Buaria, A. Pumir, and E. Bodenschatz, “Self-attenuation of extreme events in Navier-Stokes turbulence,” *Nat. Commun.* **11**, 5852 (2020).
  - [16] D. Buaria and A. Pumir, “Nonlocal amplification of intense vorticity in turbulent flows,” arXiv:2106.14370 (2021).
  - [17] D. Buaria, E. Bodenschatz, and A. Pumir, “Vortex stretching and enstrophy production in high Reynolds number turbulence,” *Phys. Rev. Fluids* **5**, 104602 (2020).
  - [18] M. Carbone and A. D. Bragg, “Is vortex stretching the main cause of the turbulent energy cascade?” *J. Fluid Mech.* **883**, R2 (2020).
  - [19] P. L. Johnson, “On the role of vorticity stretching and strain self-amplification in the turbulence energy cascade,” arXiv:2102.06844 (2021).

- [20] F. Moisy and J. Jiménez, “Geometry and clustering of intense structures in isotropic turbulence,” *J. Fluid Mech.* **513**, 111–133 (2004).
- [21] G. E. Elsinga, T. Ishihara, M. V. Goudar, C. B. Da Silva, and J. C. R. Hunt, “The scaling of straining motions in homogeneous isotropic turbulence,” *J. Fluid Mech.* **829**, 31–64 (2017).
- [22] J. Jiménez, A. A. Wray, P. G. Saffman, and R. S. Rogallo, “The structure of intense vorticity in isotropic turbulence,” *J. Fluid Mech.* **255** (1993).
- [23] H. K. Moffatt, S. Kida, and K. Ohkitani, “Stretched vortices—the sinews of turbulence; large-Reynolds-number asymptotics,” *J. Fluid Mech.* **259**, 241–264 (1994).
- [24] D. Buaria and K. R. Sreenivasan, “Dissipation range of the energy spectrum in high Reynolds number turbulence,” *Phys. Rev. Fluids* **5**, 092601(R) (2020).
- [25] R. Betchov, “An inequality concerning the production of vorticity in isotropic turbulence,” *J. Fluid Mech.* **1**, 497–504 (1956).
- [26] W. T. Ashurst, A. R. Kerstein, R. M. Kerr, and C. H. Gibson, “Alignment of vorticity and scalar gradient with strain rate in simulated Navier-Stokes turbulence,” *Phys. Fluids* **30**, 2343–2353 (1987).
- [27] A. Tsinober, M. Ortenberg, and L. Shtilman, “On depression of nonlinearity in turbulence,” *Phys. Fluids* **11**, 2291–2297 (1999).
- [28] K. K. Nomura and G. K. Post, “The structure and dynamics of vorticity and rate of strain in incompressible homogeneous turbulence,” *J. Fluid Mech.* **377**, 65–97 (1998).
- [29] M. Carbone, M. Iovieno, and A. D. Bragg, “Symmetry transformation and dimensionality reduction of the anisotropic pressure hessian,” *J. Fluid Mech.* **900**, A38 (2020).
- [30] S.B. Pope, “Lagrangian PDF methods for turbulent flows,” *Annu. Rev. Fluid Mech.* **26**, 23–63 (1994).